p-ISSN: 2301-6663, e-ISSN: 2477-250X
URL: http://ojs.ummetro.ac.id/index.php/turbo

Temperature Reduction Performance of Radiative Cooling Paint on Building Roofs

Muhammad Fuad Abdul Hakim[1*], Mohammad Alexin Putra[2], Fajar Subekti[1]

[1]Teknik Mesin, Fakultas Teknik, Universitas Merdeka Madiun
Jl. Serayu No. 79, Kota Madiun, Indonesia
[2]Teknik Mesin, Fakultas Teknologi Industri, Institut Teknologi Nasional Bandung
Jl. Phh. Mustofa No. 23, Kota Bandung, Indonesia
**Corresponding author*: muhammadfuad@unmer-madiun.ac.id

Abstract

Passive cooling technologies continue to be developed to provide a cooling effect without external energy input. One example is radiative cooling paint (RCP). RCP dissipates heat by emitting thermal radiation and reflecting solar irradiation, thereby reducing the temperature of the coated object. The temperature reduction performance of RCP is influenced by the substrate on which it is applied. Previous studies have generally not included substrates with potential applications for RCP, such as building roofs. This study aimed to evaluate the temperature reduction performance of RCP when applied to different roofing materials. RCP samples were prepared using barium sulfate pigment and applied to corrugated metal roofing, clay roof tiles, and stone-coated metal roofing, then tested under direct sunlight. The results showed that applying RCP reduced the average temperature by 6 °C (13.1%) on corrugated metal roofing, 6.4 °C (13.3%) on clay roof tiles, and 14.1 °C (24.7%) on stone-coated metal roofing.

Keywords**:** *radiative cooling paint, temperature reduction, building roofs*

1. Introduction

The need for cooling in equatorial countries, such as Indonesia, is increasing due to rising living standards. To create a comfortable environment, the air in a room exposed to direct sunlight is cooled using an air conditioner (AC). However, the use of AC requires a significant amount of external energy input (in the form of electricity), which is classified as active cooling [1]. Research [2] reported that households consume 35 - 42% more electricity when using AC. Over time, passive cooling technology has been developed, which does not require external energy input to provide a cooling effect. This passive cooling technology offers an alternative to meet cooling needs while also providing the potential for energy savings.

One of the passive cooling technologies that has been developed is radiative cooling paint (RCP) [3]. RCP is a coating capable of emitting thermal radiation through the atmosphere while reflecting solar irradiation [4] (as illustrated in Figure 1), thereby reducing the temperature of the object it covers.

Temperature reduction performance is one of the main parameters evaluated in RCP, and one of the factors influencing it is the substrate or medium on which RCP is applied [5]. In previous studies, substrates were generally selected for ease of testing, such as glass [6][7], cotton paper [8], aluminum mirrors [9], steel plate [10], silver [11], stainless steel [12], aluminum box [13] and silicon wafer [14], without considering substrates or media with potential practical applications for RCP.

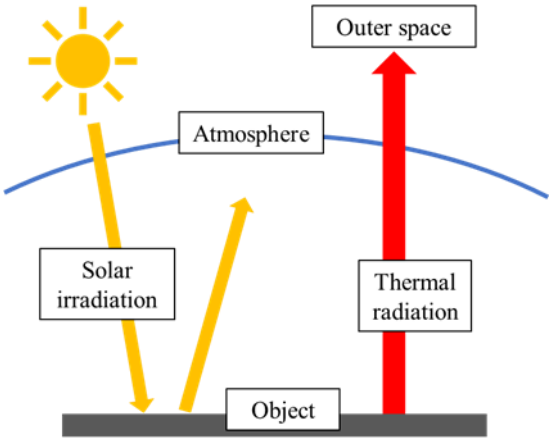

Figure 1. Illustration of radiative cooling paint

One substrate with significant potential for RCP utilization is building roofs [15]. Applying RCP to building roofs offers the possibility of passively reducing the temperature of the rooms below without additional energy consumption. Therefore,

DOI: http://dx.doi.org/10.24127/trb.v14i2.4602
Received October 2, 2025; Received in revised form December 22, 2025; Accepted December 23, 2025
Available online December 31, 2025

it is important to investigate the temperature reduction performance of RCP when applied to building roofs. The objective of this experimental study is to evaluate the temperature reduction performance of RCP on building roofs.

2. Materials and Methods

RCP samples were prepared using barium sulfate ($BaSO_4$) pigment (from PT. Smart Lab Indonesia), polymethyl methacrylate (PMMA) binder (from Himedia), and dimethylformamide (DMF) solvent (from Loba Chemie PVT. LTD). Barium sulfate pigment was selected because it demonstrated the highest temperature reduction performance compared to four other pigments (calcium carbonate, magnesium oxide, titanium dioxide, and silicon dioxide), based on the author's separate investigations.A pigment volume concentration of 60% was used in preparing the RCP samples, as this concentration was found to be optimal for barium sulfate pigment in the author's separate investigation.

The preparation process began with weighing the pigment, binder, and solvent. Based on a pigment volume concentration of 60%, the mass ratio between the pigment and binder can be calculated using Equation (1).

$$\frac{m_P}{m_B} = \frac{\rho_P \cdot PVC}{\rho_B \cdot (1 - PVC)} \quad (1)$$

where m_P represents the mass of the pigment, ρ_P the density of the pigment, m_B the mass of the binder, ρ_B the density of the binder, and PVC the pigment volume concentration.

The amount of solvent was adjusted based on the binder, with an initial mass ratio of binder to solvent set at 1:10. The solvent was poured into a beaker and placed on a hot plate stirrer. The pigment was then gradually added to the solvent to prevent agglomeration, while continuous stirring ensured proper dispersion. Next, the binder was slowly introduced while stirring until it was completely dissolved. Once fully dissolved, the RCP was ready for application. An illustration of the RCP sample preparation steps is presented in Figure 2.

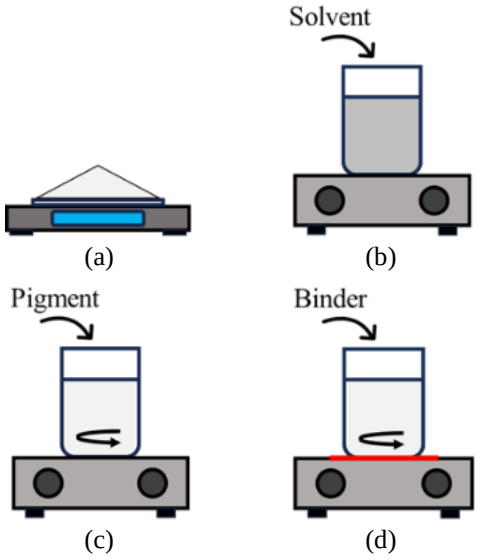

Figure 2. Steps for preparing RCP samples (a) weighing materials, (b) adding solvent, (c) adding pigment, (d) adding binder

Figure 3. (a) corrugated metal roofing, (b) clay roof tiles, and (c) stone-coated metal roofing

To determine the temperature reduction performance of RCP when applied to building roofs, the RCP sample was applied to three types of roofing materials: corrugated metal roofing, clay roof tiles, and stone-coated metal roofing, as shown in Figure 3. These roof types were selected because they are commonly used in Indonesia.

After each type of roof was coated with RCP, testing was conducted under direct sunlight by comparing coated and uncoated roofs, as shown in Figure 4. The testing was limited to a single piece or a small section of each roof type, rather than a full-scale house roof with a large area. A whole clay roof tile was used, while the corrugated metal roofing and stone-coated metal roofing were cut to a size of 17 cm x 10 cm to optimize the use of materials for RCP preparation.

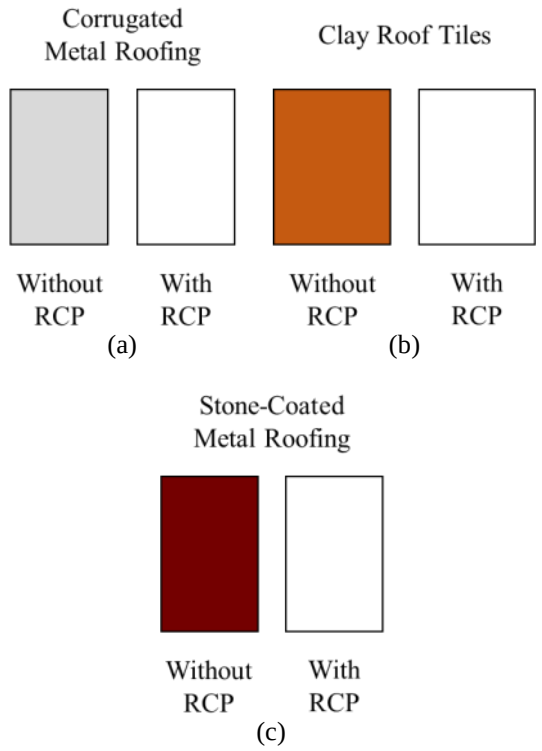

Figure 4. Illustration of (a) corrugated metal roofing, (b) clay roof tiles, (c) stone-coated metal roofing coated with RCP and uncoated for testing

The testing was conducted during the daytime, from 09:30 AM to 02:30 PM, in an open area when solar irradiation was high. The data collected included the backside temperature of the corrugated metal roofing, clay roof tiles, and stone-coated metal roofing, both with and without RCP coating. Data were recorded every two minutes throughout the testing period. The collected data were then processed using Equation (2) to determine the average temperature reduction achieved by RCP on the three roof types, providing an overview of its temperature reduction performance.

$$\Delta T_{Avg} = \frac{1}{n}\sum_{i=1}^{n}(T_{With\ RCP,\ i} - T_{Without\ RCP,\ i}) \quad (2)$$

where ΔT_{Avg} is the average temperature reduction, n is the number of temperature measurements, and T is the backside surface temperature of the building roofs.

3. Result and Discussion

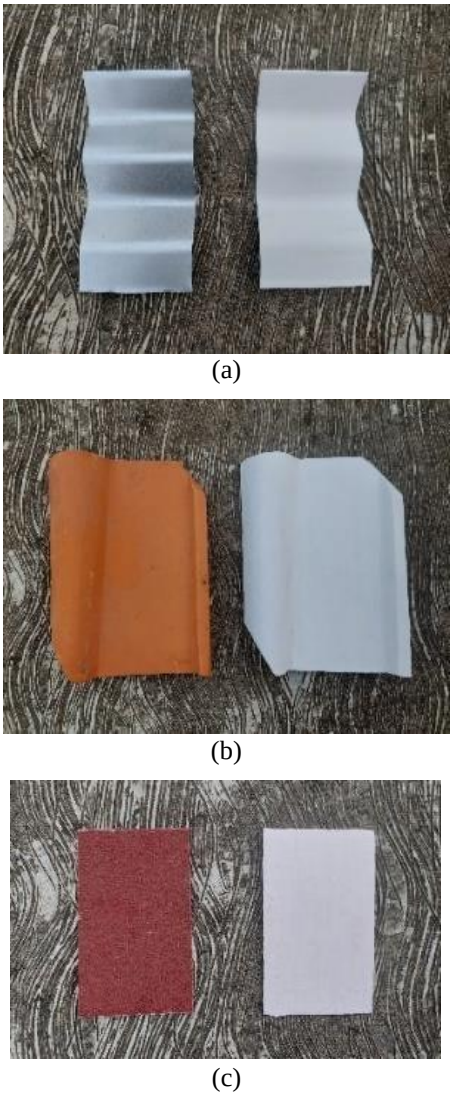

Figure 5. (a) corrugated metal roofing, (b) clay roof tiles, (c) stone-coated metal roofing, coated with RCP and uncoated

Figure 5 shows the three types of building roofs, corrugated metal roofing,

clay roof tiles, and stone-coated metal roofing, both with and without RCP coating.

The testing under direct sunlight is presented in Figure 6.

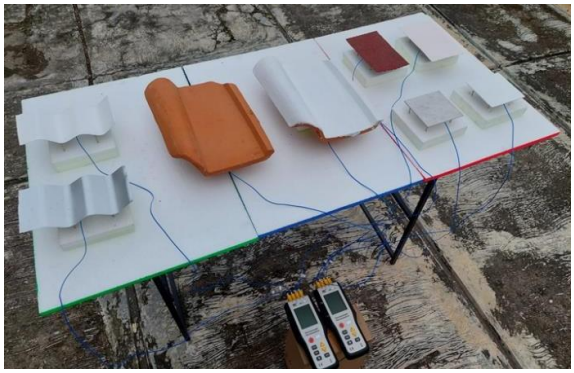

Figure 6. Testing under direct sunlight

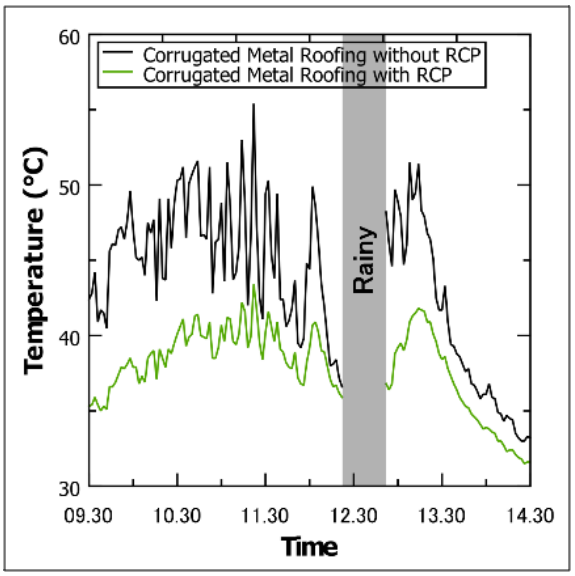

(a)

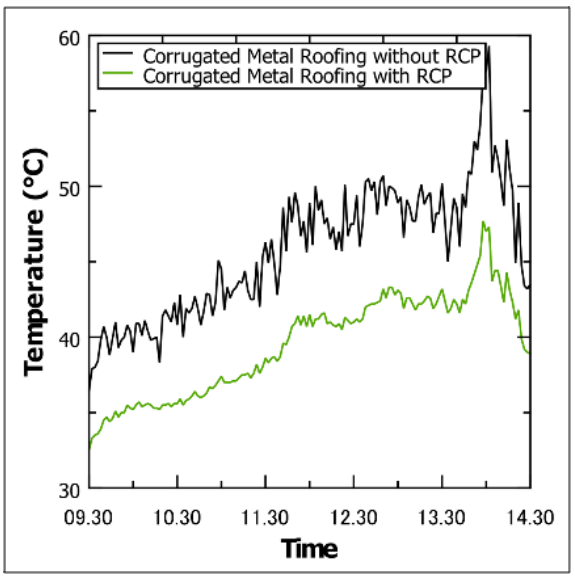

(b)

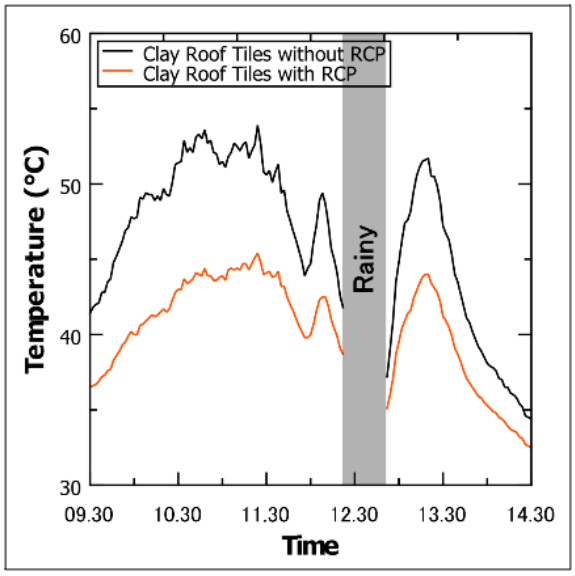

(c)

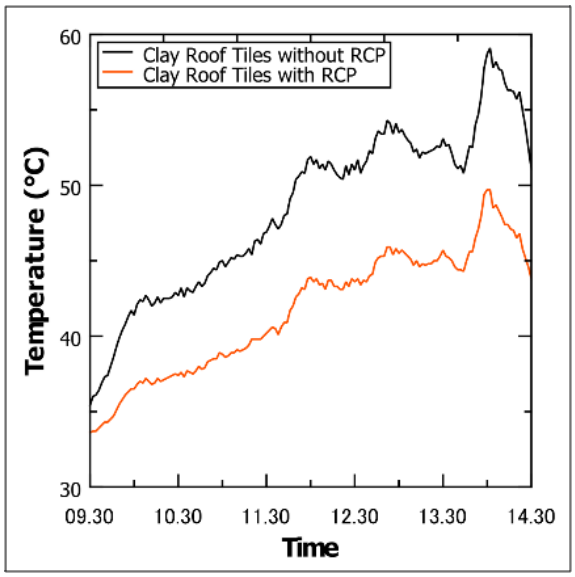

(d)

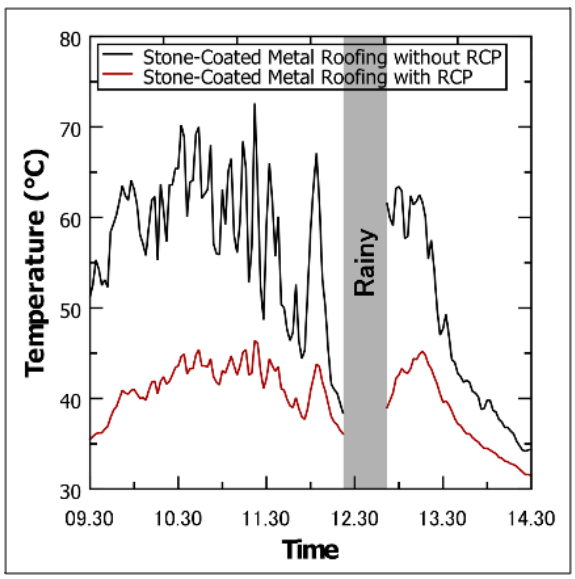

(e)

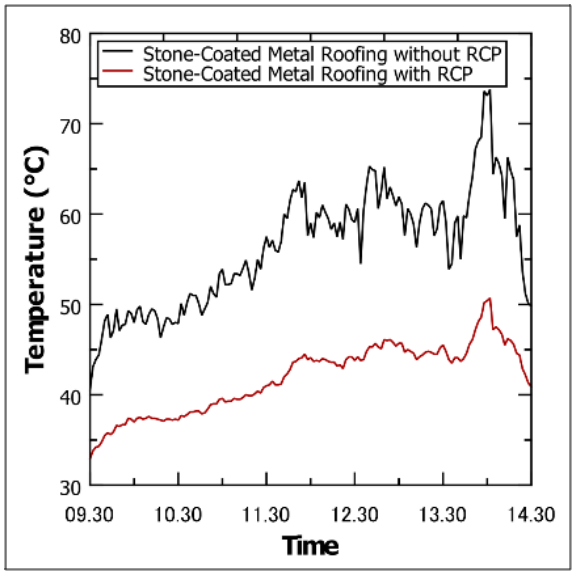

(f)

Figure 6. Temperature data from the testing results (day 1 & 2) for (a-b) corrugated metal roofing, (c-d) clay roof tiles, and (e-f) stone-coated metal roofing

The backside temperature data of the three roof types from the testing results are presented in Figure 7. The tests were conducted twice, on December 7 and 8, 2024.

The average temperature from the test results on corrugated metal roofing, clay roof tiles, and stone-coated metal roofing is presented in Table 1.

Table 1. The average temperature of corrugated metal roofing, clay roof tiles & stone-coated metal roofing

Roof type	Average temperature	
	Without RCP	With RCP
Corrugated metal roofing	44.7 ºC	38.7 ºC
Clay roof tiles	47.5 ºC	41.1 ºC
Stone-coated metal roofing	55.1 ºC	41.0 ºC

Before discussing the temperature reduction performance of RCP, it can be observed from Table 1 that stone-coated metal roofing without RCP has the highest average temperature compared to corrugated metal roofing and clay roof tiles. Stone-coated metal roofing is made of thin metal sheets (typically galvalume steel or zincalume) with a sand layer on top. These thin metal sheets have high thermal conductivity (around 50 W/m.K), allowing heat to be quickly conducted throughout the material. The sand layer, on the other hand, has low thermal conductivity (approximately 0.2 - 0.7 W/m.K [16]) and a high specific heat capacity (around 703 J/kg.K [16]), along with low diffusivity. As a result, heat from solar irradiation tends to be stored for a longer period in the sand layer. This leads to an accumulation or trapping of heat between the thin metal sheets and the sand layer, causing stone-coated metal roofing to have a relatively higher overall temperature.

Corrugated metal roofing has relatively high thermal conductivity (around 60 - 65 W/m.K [17][18]) and relatively low specific heat capacity (around 465 J/kg.K [17]), with relatively high diffusivity. This allows it to absorb and release heat quickly, making it more sensitive to environmental changes, without the heat accumulation or trapping observed in stone-coated metal roofing. This behavior can be seen in the temperature graph from the testing results in Figure 7a-b, where the temperature of corrugated metal roofing tends to fluctuate more.

In contrast, clay roof tiles have low thermal conductivity (around 0.7 W/m.K [19]) and high specific heat capacity (around 880 J/kg.K [20]), with low diffusivity. As a result, they absorb and release heat more slowly and are relatively less sensitive to environmental changes. This is evident in the temperature graph in Figure 7c-d, where the temperature of clay roof tiles fluctuates less. However, heat tends to be stored and retained for a longer period, causing the overall temperature of clay roof tiles to be higher than that of corrugated metal roofing.

From the temperature reduction performance of RCP, it can be observed from Figure 7 that corrugated metal roofing, clay roof tiles, and stone-coated metal roofing coated with RCP have lower temperatures compared to those without

RCP. Considering the temperature reduction, defined as the difference between the temperatures of roofs coated with RCP and those without (used as the reference), the results are presented in Figure 8.

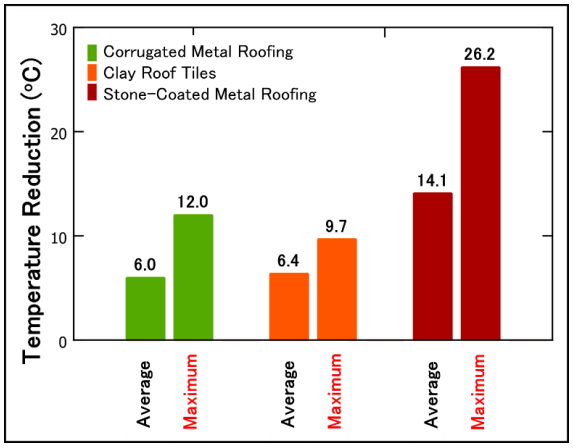

Figure 8. Average and maximum temperature reduction results from the testing

RCP can reduce the temperature of the object it coats due to factors associated with the pigment, in this case $BaSO_4$. The factors associated with the pigment include the band gap, refractive index, and pigment color.

The band gap represents the minimum photon energy required to transfer an electron from the valence band to the conduction band, which is related to a material's ability to absorb solar irradiation. If the band gap of a material is smaller than the photon energy carried by solar irradiation, the material will more easily absorb solar irradiation [21]. Conversely, if the band gap of a material is larger than the photon energy carried by solar irradiation, the material will be less able to absorb solar irradiation. Solar irradiation reaching the Earth's surface carries photon energies in the range of 0.5 eV–4.1 eV (wavelengths of 0.3–2.5 µm). $BaSO_4$ pigment has a band gap value of approximately 6 eV [22], which is higher than the photon energy carried by solar irradiation, and therefore tends to be less able to absorb solar irradiation.

Then, the refractive index affects the extent to which light/electromagnetic waves are bent when passing through a medium. The higher the refractive index, the more the light/electromagnetic waves, or in this case solar irradiation, are bent, making solar irradiation more effectively reflected. $BaSO_4$ pigment has a relatively high refractive index of about 1.6 [23].

The color of an object or surface affects its absorptivity toward solar irradiation. $BaSO_4$ pigment has a white appearance, where the white color has the lowest absorptivity toward solar irradiation compared to other colors [24].

From Figure 8, it can be seen that the highest temperature reduction achieved by RCP occurred on stone-coated metal roofing, with average and maximum reductions of 14.1 °C and 26.2 °C, respectively. The use of RCP is considered more effective on stone-coated metal roofing, as the average temperature reduction is approximately twice that observed on corrugated metal roofing (12.0 °C) and clay roof tiles (9.7 °C). This can be explained by the fact that a portion of the incoming solar irradiation on stone-coated metal roofing is reflected by the RCP, thereby reducing the amount of heat stored in the sand/stone layer and resulting in a significant temperature reduction.

When expressed as a percentage, the average temperature reduction, the difference between RCP coated and uncoated roofs, is 13.1% for corrugated metal roofing, 13.3% for clay roof tiles, and 24.7% for stone-coated metal roofing. For corrugated metal roofing and clay roof tiles, the results indicate similar average reductions. Although the temperature reductions on these two roof types are not as large as those observed for stone-coated metal roofing, the use of RCP on both remains worthwhile to consider.

4. Conclusion

Based on the test results under direct sunlight using an RCP sample made from barium sulfate pigment with a pigment volume concentration of 60%, applied to corrugated metal roofing, clay roof tiles, and stone-coated metal roofing compared to their uncoated counterparts, the average

temperature reductions obtained were 6.0 °C (13.1%) for corrugated metal roofing, 6.4 °C (13.3%) for clay roof tiles, and 14.1 °C (24.7%) for stone-coated metal roofing.

References

[1] P. Dwivedi, K. Sudhakar, A. Soni, E. Solomin, and 1 Kirpichnikova, "Advanced Cooling Techniques of P.V. Modules: A State of Art," *Case Stud. Therm. Eng.*, vol. 21, pp. 1–17, 2020, doi: 10.1016/j.csite.2020.100674.

[2] T. Randazzo, E. De Cian, and M. N. Mistry, "Air conditioning and electricity expenditure: The role of climate in temperate countries," *Econ. Model.*, vol. 90, pp. 273–287, Aug. 2020, doi: 10.1016/j.econmod.2020.05.001.

[3] J. Mandal, Y. Yang, N. Yu, and A. P. Raman, "Paints as a Scalable and Effective Radiative Cooling Technology for Buildings," *Joule*, vol. 4, no. 7, pp. 1350–1356, Jul. 2020, doi: 10.1016/j.joule.2020.04.010.

[4] M. Chen, D. Pang, X. Chen, H. Yan, and Y. Yang, "Passive daytime radiative cooling: Fundamentals, material designs, and applications," *EcoMat*, vol. 4, no. 1, Jan. 2022, doi: 10.1002/eom2.12153.

[5] W. R. Joseph, J. Y. Tan, A. K. Koyande, I. Khoiroh, J. Joynson, and S. Willis, "Subambient passive radiative cooling effects of barium sulfate and calcium carbonate paints under Malaysia's tropical climate," *Environ. Sci. Adv.*, vol. 2, no. 12, pp. 1662–1679, 2023, doi: 10.1039/D3VA00161J.

[6] H. Lim, D. Chae, S. Son, J. Ha, and H. Lee, "CaCO3 micro particle-based radiative cooling device without metal reflector for entire day," *Mater. Today Commun.*, vol. 32, p. 103990, Aug. 2022, doi: 10.1016/j.mtcomm.2022.103990.

[7] M. M. S. Altamimi, U. Saeed, and H. Al-Turaif, "BaSO4/TiO2 Microparticle Embedded in Polyvinylidene Fluoride-Co-Hexafluoropropylene/Polytetrafluoroethylene Polymer Film for Daytime Radiative Cooling," *Polymers (Basel).*, vol. 15, no. 19, p. 3876, Sep. 2023, doi: 10.3390/polym15193876.

[8] A. Felicelli *et al.*, "Efficient radiative cooling of low-cost $BaSO_4$ paint-paper dual-layer thin films," *Nanophotonics*, vol. 13, no. 5, pp. 639–648, Mar. 2024, doi: 10.1515/nanoph-2023-0642.

[9] T. Suichi, A. Ishikawa, Y. Hayashi, and K. Tsuruta, "Performance limit of daytime radiative cooling in warm humid environment," *AIP Adv.*, vol. 8, no. 5, May 2018, doi: 10.1063/1.5030156.

[10] S. Atiganyanun and P. Kumnorkaew, "Effects of pigment volume concentration on radiative cooling properties of acrylic-based paints with calcium carbonate and hollow silicon dioxide microparticles," *Int. J. Sustain. Energy*, vol. 42, no. 1, pp. 612–626, Dec. 2023, doi: 10.1080/14786451.2023.2221082.

[11] H. O. Okoro *et al.*, "Preliminary Experimental Performance Assessment of Ultra-White Barium Sulphate for Sub-Ambient Radiative Cooling in Abuja, Nigeria," *Int. J. Adv. Sci. Eng.*, vol. 10, no. 3, pp. 3508–3516, Mar. 2024, doi: 10.29294/IJASE.10.3.2024.3508-3516.

[12] D. F. A. Putra, U. Qazi, P.-H. Chen, and S.-J. Shih, "Preparation and Characterization of SiO2-PMMA and TiO2-SiO2-PMMA Composite Thick Films for Radiative Cooling Application," *J. Compos. Sci.*, vol. 8, no. 11, p. 453, Nov. 2024, doi: 10.3390/jcs8110453.

[13] B. R. Mishra, S. Sundaram, and K. Sasihithlu, "Design of Radiative Cooling Paint Coating and Insights Into Its Sub-ambient Cooling

Behaviour," *ArXiv Prepr.*, 2024, doi: https://doi.org/10.48550/arXiv.2401.11765.

[14] P. Das, S. Rudra, K. C. Maurya, and B. Saha, "Ultra-Emissive MgO-PVDF Polymer Nanocomposite Paint for Passive Daytime Radiative Cooling," *Adv. Mater. Technol.*, vol. 8, no. 24, Dec. 2023, doi: 10.1002/admt.202301174.

[15] A. Aili *et al.*, "Passive daytime radiative cooling: Moving beyond materials towards real-world applications," *Next Energy*, vol. 3, p. 100121, Apr. 2024, doi: 10.1016/j.nxener.2024.100121.

[16] S. Tetteh, G. Juul, M. Järvinen, and A. Santasalo-Aarnio, "Improved effective thermal conductivity of sand bed in thermal energy storage systems," *J. Energy Storage*, vol. 86, p. 111350, May 2024, doi: 10.1016/j.est.2024.111350.

[17] D. Boureima, M. K. Thierry Sikoudouin, O. Emmanuel, H. Koami Soulemane, and B. Dieudonn Joseph, "Theoretical Study of a Thermal Photovoltaic Hybrid Solar Collector," *Indian J. Sci. Technol.*, vol. 11, no. 43, pp. 1–9, Nov. 2018, doi: 10.17485/ijst/2018/v11i43/132133.

[18] O. Nurhilal, N. M. Farizan, F. Rahman, and S. Setianto, "Enhancing water heater efficiency with aluminum and zinc-coated steel systems for energy solutions," *Heliyon*, vol. 10, no. 16, p. e35682, Aug. 2024, doi: 10.1016/j.heliyon.2024.e35682.

[19] M. Ariyadasa and U. Adikary, "Investigating the Physical, Mechanical and Thermal Properties of Common Roofing Materials in Sri Lanka," *NBRO Sysposium 2015 "Innovations Resilient Environ.*, no. December, 2015.

[20] T. L. Bergman, A. S. Lavine, F. P. Incropera, and D. P. Dewitt, *Fundamentals of Heat and Mass Transfer*, Seventh Ed. John Wiley & Sons, Inc, 2011.

[21] B. R. Sutherland, "Solar Materials Find Their Band Gap," *Joule*, vol. 4, no. 5, pp. 984–985, May 2020, doi: 10.1016/j.joule.2020.05.001.

[22] X. Li, J. Peoples, P. Yao, and X. Ruan, "Ultrawhite $BaSO_4$ Paints and Films for Remarkable Daytime Subambient Radiative Cooling," *ACS Appl. Mater. Interfaces*, vol. 13, no. 18, pp. 21733–21739, May 2021, doi: 10.1021/acsami.1c02368.

[23] R. C. Ropp, "Group 16 (O, S, Se, Te) Alkaline Earth Compounds," in *Encyclopedia of the Alkaline Earth Compounds*, Elsevier, 2013, pp. 105–197. doi: 10.1016/B978-0-444-59550-8.00003-X.

[24] J. Paminto and I. Yulianti, "The Effect of Surface Color on the Absorption of Solar Radiation Physics Communication," *Phys. Comm*, vol. 5, no. 1, pp. 27–32, 2021, [Online]. Available: http://journal.unnes.ac.id/nju/index.php/pc